*Proceedings of the 5th International Conference on Inverse Problems in Engineering: Theory and Practice, Cambridge, UK, 11-15th July 2005*

# GAS TEMPERATURE IDENTIFICATION FOR THE SIMULATION OF ELECTRIC FAULT ARC TESTS

P. STEINHORST, B. HOFMANN, A. MEYER and W. WEINELT
Faculty of Mathematics, Chemnitz University of Technology, D-09107 Chemnitz, Germany
e-mail: pest@mathematik.tu-chemnitz.de b.hofmann@mathematik.tu-chemnitz.de
a.meyer@mathematik.tu-chemnitz.de w.weinelt@mathematik.tu-chemnitz.de

**Abstract -** In this paper we present some mathematical model and some numerical approach for a computer-based simulation of electric fault arc tests. In particular, we replace the complex initial-boundary value problem of heat transfer in arc tests by using a one-dimensional model based on a purely time-dependent temperature function $G(t)$ of hot gas in a neighborhood of the arc. We are especially interested in the identification of this parameter function $G$ from temperature measurements at a defined distance to the arc during some time interval, where a simplified test procedure is exploited for obtaining temperature data. This ill-posed inverse problem of determining $G$ is investigated in detail. We present a least-squares solution indicating the ill-posedness effect by strong oscillations and compare a solution from Tikhonov regularization with a solution from a descriptive regularization approach. A sensitivity study completes the paper.

## 1. INTRODUCTION AND TECHNICAL BACKGROUND

Fault arc tests are performed in textile research and certification of protective clothes. Textile protection is used for human people working on electric installations, where a potential risk of fault arc accidents occurs causing human injury with heavy burns. There are different arc test methods in the international standardization, [6]. One special European test is the so called CENELEC test, prescribed in the pre-standard ENV 50354:2001. This box-arc test method described in [8] contains a visual assessment (after flaming, hole formation, shrinking etc.) as a qualitative criterion and was extended and improved by including additionally a quantitative measurement of temperatures in order to get information about the really transmitted energy. The schematic test arrangement of such a complemented test is shown in Figure 1.

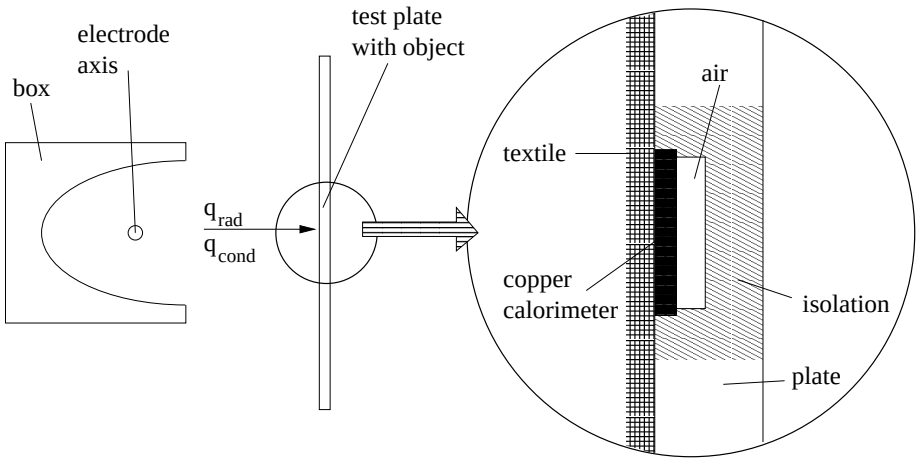


Figure 1: Schematic test arrangement.

An electric arc is fired between two vertically arranged electrodes in a test circuit of defined voltage (AC). After the burning-time interval of $t_p = 0.5s$ the arc is switched off. A surrounding box focuses thermal arc effects in direction to a test plate with test object, which is arranged in a defined distance to the electrodes. The object consists of a variable number of textile layers stretched onto the test plate and of a skin-simulating copper calorimeter embedded by an isolating block in the test plate as shown in Figure 1. The calorimeter is connected with a thermocouple, and so the calorimeter temperature is measured from the arc ignition ($t = 0$) until the end of measuring time $t_{\text{end}} = 30s$.

A numerical simulation of calorimetric arc effects based on the complemented test method was realized at the Chemnitz University of Technology in cooperation with the Saxon Textile Research Institute (STFI) and the Ilmenau University of Technology, [9]. For the mathematical simulation of the test we used a mathematical model, which will be described below in section 2. In the model building process we have replaced the very complex structure of the system formed by arc, heated gas and reflecting box by a gas temperature function depending on time. The determination of this parameter function which influences the result of test simulation in an essential manner leads to the inverse problem discussed in this paper. Before handling the stable approximate solution of this inverse problem in section 4, we briefly mention the numerical solution of the associated forward problem in section 3.

## 2. THE MATHEMATICAL MODEL

We have simplified the whole test arrangement in form of a locally one-dimensional heat equation problem, where the gas temperature near the arc is assumed to be a function $G(t)$ of time $t$ only. The spatial $x$-axis lies orthogonal to the surface of the test object (plate with or without textile) such that heat fluxes of interest here are directed along the $x$-axis. Figure 2 shows the modeled object with three textile layers as an example.

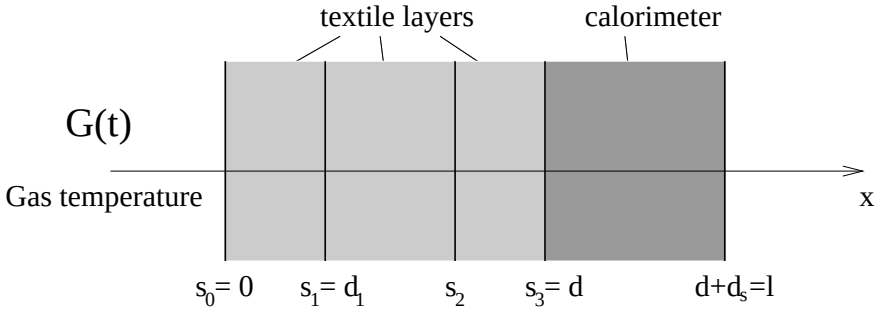


Figure 2: 1D-model of the object.

We use the following notations:

| | |
|---|---|
| $x$ | 1D local coordinate, $x \in \Omega = [0, l]$, |
| $t$ | time, $t \in [0, t_{\text{end}}]$, |
| $u = u(x, t)$ | temperature in the object, |
| $G = G(t)$ | temperature of the hot gas, |
| $C^A(x, t, u(x, t))$ | apparent heat capacity (modified, specified by volume), |
| $\kappa(x, u(x, t))$ | thermal conductivity, |
| $f_{\text{rad}}(x, t, G(t), u(0, t))$ | radiation heat source term, |
| $h_0, h_s$ | heat transfer coefficients. |

The occurring temperatures $u$ and $G$ are seen as relative temperatures with respect to the ambient temperature which is defined as $T_{\text{amb}} = 0$. However, for modeling the radiation absolute temperatures are needed. For this case, sometimes the assumed room temperature of $T_0 = 300K$ is added to the relative temperatures.

Then, the temperature distribution $u = u(x, t),\ x \in [0, l],\ t \in [0, t_{\text{end}}]$ under consideration is the solution of the initial-boundary value problem to the heat equation

$$C^A(x, t, u(x, t))\frac{\partial u}{\partial t} - \frac{\partial}{\partial x}\left(\kappa(x, u(x, t))\frac{\partial u}{\partial x}\right) = f_{\text{rad}}(x, t, G(t), u(0, t)) \qquad (x \in (0, l),\ t \in (0, t_{\text{end}}]) \quad (1)$$

with boundary conditions

$$-\kappa(0, u(0, t))\frac{\partial u(x, t)}{\partial x}\bigg|_{x=0} = h_0(G(t) - u(0, t)) \qquad (t \in (0, t_{\text{end}}]), \quad (2)$$

$$\kappa(l, u(l, t))\frac{\partial u(x, t)}{\partial x}\bigg|_{x=l} = h_s(T_{\text{amb}} - u(l, t)) \qquad (t \in (0, t_{\text{end}}]) \quad (3)$$

and initial condition

$$u(x, 0) = 0 \qquad (x \in [0, l]). \quad (4)$$

Heat effects enter the model by boundary conditions in form of heat transition and by the source term $f_{\mathrm{rad}}$ in the differential equation indicating the effect of radiation.

In order to calculate $u(x,t)$ from (1) – (4) the knowledge of the gas temperature $G(t)$ is required. For the determination of this function temperature measurement data from calibration tests are used. The calibration test is performed without textile layers, where the object consists of the test plate with the calorimeter only. For this reason, we use the simplified version

$$C_{\mathrm{Cu}}\frac{\partial u}{\partial t}-\frac{\partial}{\partial x}\left(\kappa_{\mathrm{Cu}}\frac{\partial u}{\partial x}\right)=f_{\mathrm{rad}}(x,t,G(t),u(0,t)) \qquad (x\in(0,l),\ t\in(0,t_{\mathrm{end}}]) \tag{5}$$

of heat equation. Here the volumetric heat capacity $C_{\mathrm{Cu}}$ and the thermal conductivity $\kappa_{\mathrm{Cu}}$ are assumed to be constant. Note that $\kappa_{\mathrm{Cu}}$ in fact depends on the temperature, but the measured and simulated temperatures of the copper calorimeter are from the temperature interval $[20°C, 110°C]$ (see section 4). For this range, however, the thermal conductivity of copper is nearly a constant (see, e.g. [5, Chap. 6-12, Table 6-18]). The radiation source term has the structure

$$f_{\mathrm{rad}}(x,t,G(t),u(0,t))=\gamma e^{-\gamma x}\left(q_a(t)+\beta_{\mathrm{Gas}}(G(t)+T_0)^4-\beta_{\mathrm{Obj}}\left((u(0,t)+T_0)^4-T_0^4\right)\right) \tag{6}$$

for $x\in(0,l)$ and $t\in(0,t_{\mathrm{end}}]$ with positive constants $\beta_{\mathrm{Gas}},\beta_{\mathrm{Obj}}$ and $\gamma$; $q_a$ is a given source term of the burning arc. The boundary conditions (2) – (3) are reduced to

$$-\kappa_{\mathrm{Cu}}\frac{\partial u(x,t)}{\partial x}\bigg|_{x=0}=h_0(G(t)-u(0,t)) \qquad (t\in[0,t_{\mathrm{end}}]) \tag{7}$$

and

$$\kappa_{\mathrm{Cu}}\frac{\partial u(x,t)}{\partial x}\bigg|_{x=l}=h_s(T_{\mathrm{amb}}-u(l,t)) \qquad (t\in[0,t_{\mathrm{end}}])\ . \tag{8}$$

The inverse problem under consideration here aims at finding the gas temperature function $G(t)$ from given data $u(l,t)$ for $t\in[0,t_{\mathrm{end}}]$ solving the problem (5) – (8) with initial condition (4).

In this special situation the model contains nonlinearities only in the radiation source term. The forward operator $F$ mapping the function $G(t)$ to be determined to the observable temperature function $u(l,t)\,(t\in[0,t_{\mathrm{end}}])$ is continuous and small changes in $G$ cause only small changes in $u$. This is a consequence of well-known stability assertions with respect to perturbations in the source term and in the boundary condition of parabolic initial-boundary value problems (see [2, Chapter 5, §3 (Lemma 2)] for a $C$-space setting and [7, Chapter IV, Theorem 9.1] for an $L^p$-space setting). The well-known theory of parabolic equations is applicable, since the source function $f_{\mathrm{rad}}$ in (5) is smooth and continuously differentiable with respect to $G$ and the mean value theorem provides appropriate parabolic initial-boundary value problems in which only the increment $\triangle G$ of the gas temperature function occurs as a perturbation in the source term and in the boundary condition.

## 3. NUMERICAL APPROXIMATION OF THE FORWARD PROBLEM

In this section, we roughly outline the approximate numerical solution of the initial-boundary value problem (1) – (4) that characterizes the forward problem which is to be solved for simulating the effects of fault arc accidents if textile material is used in order to avoid heavy burns. Here, the gas temperature $G(t)$ is assumed to be known. The time- and space-dependence and the nonlinearities in $C^A$, $\kappa$ and $f_{\mathrm{rad}}$ require some special treatment.

We are going to use a classical time–stepping algorithm such as backward Euler or the Crank–Nicolson scheme: Let $\tau$ denote the time increment and $u^n(x)$ the approximate solution at time step $t_n$, then for $t_{n+1}=t_n+\tau$ we have to solve the nonlinear differential equation

$$C^A(x,t_n^*,u^{n,*})\frac{u^{n+1}-u^n}{\tau}-\frac{\partial}{\partial x}\left((\kappa(x,u^{n,*})\frac{\partial}{\partial x}u^{n,*}\right)=f_{\mathrm{rad}}\left(x,t_n^*,G(t_n^*),u^{n,*}(0)\right) \qquad (x\in(0,l)) \tag{9}$$

in space with boundary conditions

$$\begin{aligned}-\kappa\left(0,u^{n+1}(0)\right)\tfrac{\partial}{\partial x}u^{n+1}(0)&=h_0\left(G(t_n^*)-u^{n+1}(0)\right),\\ \kappa\left(l,u^{n+1}(l)\right)\tfrac{\partial}{\partial x}u^{n+1}(l)&=h_s\left(T_{\mathrm{amb}}-u^{n+1}(l)\right).\end{aligned}$$

Here, $t_n^*=(1-\sigma)t_n+\sigma t_{n+1}=t_n+\sigma\tau$ and $u^{n,*}(x)=(1-\sigma)u^n(x)+\sigma u^{n+1}(x)$ describe the approximation of $u(x,t_n+\sigma\tau)$. The choice $\sigma=0$ belongs to the simple explicit Euler scheme, which is known to be

stable only for very small time step restrictions. So we prefer for simplicity the backward Euler scheme with $\sigma = 1$. Note that $\sigma = \frac{1}{2}$ would yield the Crank–Nicolson scheme.

For the discretization in space, we can use linear finite elements. Here, the fact of one space dimension leads to stiffness and mass matrices that are tridiagonal and each linear system with such a matrix is solved with optimal arithmetical complexity (proportional to the number of unknowns). So, we can use a very fine mesh without problems of calculation time. From this reason it seems to be convenient to focus on linear elements. Let $x_i = ih$ be the discretization points and $\varphi_i(x)$ the hat–functions (linear in each interval $[x_{i-1}, x_i]$ and $\varphi_i(x_j) = \delta_{ij}$) with $h = l/N$ and $i = 0, \ldots, N$. The equidistance of the points $x_i$ is not necessary. Therefore, we assume $x = s_0,\ x = s_1,\ x = s_2,\ \ldots,\ x = d$ (see Figure 2) to coincide with some of the nodal points $x_j$. Then, the weak formulation of (9) reads as:
Find $u^{n+1}(x) \in H^1(0,l)$ with

$$\begin{aligned} &\langle C^A u^{n+1}, v\rangle + \tau\langle \kappa \frac{\partial}{\partial x} u^{n+1}, \frac{\partial}{\partial x} v\rangle + \tau v(0) h_0 u^{n+1}(0) + \tau v(l) h_s u^{n+1}(l) \\ &= \tau\langle f, v\rangle + \langle C^A u^n, v\rangle + v(0)\tau h_0 G(t_{n+1}) + v(l)\tau h_s T_{\text{amb}} \quad \forall v \in H^1(0,l) \end{aligned} \tag{10}$$

Here, $\langle u, v\rangle = \int_0^l u \cdot v \, dx$ stands for the $L_2$–inner product of functions over $[0,l]$. Note that $C^A$, $\kappa$ and $f$ contain the nonlinearities associated with its dependence on the solution $u^{n+1}$ of the actual time step. For the full implicit scheme, we have

$$\begin{aligned} C^A &= C^A(x, t_{n+1}, u^{n+1}) \\ \kappa &= \kappa(x, u^{n+1}) \\ f(x) &= f_{\text{rad}}(x, t_{n+1}, G(t_{n+1}), u^{n+1}(0)) \ . \end{aligned}$$

With $u^{n+1}(x) = \sum_{i=0}^{N} \underline{u}_i^{n+1} \varphi_i(x)$ we represent the finite element approximation of this function by a unique vector $\underline{u}^{n+1} = (\underline{u}_i^{n+1})_{i=0}^N \in \mathbb{R}^{N+1}$. Then (10) coincides with the non–linear system of $N+1$ equations

$$M(\underline{u}^{n+1})\underline{u}^{n+1} + \tau K(\underline{u}^{n+1})\underline{u}^{n+1} = \tau \underline{b}(\underline{u}^{n+1}) + M(\underline{u}^{n+1})\underline{u}^n \tag{11}$$

with the tridiagonal matrices $M$ and $K$, which depend on the solution as

$$\begin{aligned} M(\underline{u}) &= \left( \langle C^A(u)\varphi_j, \varphi_i\rangle \right)_{i,j=0}^N , \\ K(\underline{u}) &= \left( \langle \kappa(u) \frac{\partial}{\partial x}\varphi_j, \frac{\partial}{\partial x}\varphi_i\rangle + h_0 \varphi_j(0)\varphi_i(0) + h_s \varphi_j(l)\varphi_i(l) \right)_{i,j=0}^N \end{aligned}$$

and

$$\underline{b}(\underline{u}) = \left( \langle f(u), \varphi_i\rangle + \varphi_i(0) h_0 G(t_{n+1}) + \varphi_i(l) h_s T_{\text{amb}} \right)_{i=0}^N .$$

For the solution of the non–linear vector equation (11) we may use some iteration steps of the following process: With $\underline{v}^{(0)} = \underline{u}^n$, iterate (solve for $\underline{v}^{(k)}$):

$$\left( M(\underline{v}^{(k-1)}) + \tau K(\underline{v}^{(k-1)}) \right) \underline{v}^{(k)} = \tau \underline{b}(\underline{v}^{(k-1)}) + M(\underline{v}^{(k-1)})\underline{u}^n . \tag{12}$$

Each iteration requires the quick optimal solution of a tridiagonal linear system of equations. After some steps ($k = 1, \ldots, k^{\text{end}}$) we set $\underline{u}^{n+1} := \underline{v}^{(k^{\text{end}})}$. We have used $k^{\text{end}} = 5$ successfully in case studies. The choice $k^{\text{end}} = 1$ coincides with the explicit Euler scheme ($\sigma = 0$ in (9)). So, for $k^{\text{end}} > 1$ each step of the iteration has a tendency to approach the full implicit Euler scheme. The matrices $M(\underline{u}) + \tau K(\underline{u})$ are symmetric positive definite tridiagonal, hence the solution of the linear systems uses a special variant of the Cholesky decomposition for tridiagonal matrices.

Note that the described approximation is also used to solve the forward problem (5) – (8) which is required for the identification of $G$. In this simplified situation constant material values lead to constant matrices $K$ and $M$.

## 4. THE INVERSE PROBLEM AND VARIANTS OF ITS SOLUTION

For the inverse problem aimed at finding the gas temperature $G(t)$ ($t \in [0, t_{\text{end}}]$) real measurements $y^*(t)$ ($t \in [0, t_{\text{end}}]$) of the output temperature $y(t) = u(l, t)$ ($t \in [0, t_{\text{end}}]$) can be exploited as data, where the simplified version of the arc test without additional textile material was performed for providing such data. The used constants based on the technological literature (for details see also [8] and [9]) are specified by the following list:

$$\begin{aligned} l &= 1.6mm = d_s, \\ \kappa_{\text{Cu}} &= 392W \cdot m^{-1}K^{-1}, \\ C_{\text{Cu}} &= 3.4265 \cdot 10^6 J \cdot m^{-3}K^{-1}, \\ \gamma &= 2.05 \cdot 10^5 m^{-1}, \\ q_a(t) &= 7.055 \cdot 10^4 W \cdot m^{-2} \cdot \chi_{[0,t_p]}(t), \\ \beta_{\text{Gas}} &= 1.114 \cdot 10^{-9} W \cdot m^{-2}K^{-4}, \\ \beta_{\text{Obj}} &= 4.72 \cdot 10^{-8} W \cdot m^{-2}K^{-4}, \\ h_0 &= 40W \cdot m^{-2}K^{-1}, \\ h_s &= 15W \cdot m^{-2}K^{-1}. \end{aligned}$$

Here, $\chi_{[a,b]}$ is the characteristic function with respect to the interval $[a, b]$. The values $\beta_{\text{Gas}}$ and $\beta_{\text{Obj}}$ are products of dimensionsless factors with the Stefan-Boltzmann constant.

If we denote by $F : G \mapsto y$ the nonlinear operator with domain $D$ that expresses the parameter-to-data map, so the inverse problem can be considered as the solution of an operator equation

$$F(G) = y \qquad (G \in D) \tag{13}$$

taking into account that the data $y^*$ represent a noisy version of the exact right-hand side $y$. Figure 3 shows this data $y^*$ really observed during the simplified test. The domain $D$ under consideration may contain all available a priori information on the time-dependent behavior of $G$ including box-constraints as well as monotonicity of gas temperature on some subintervals of time.

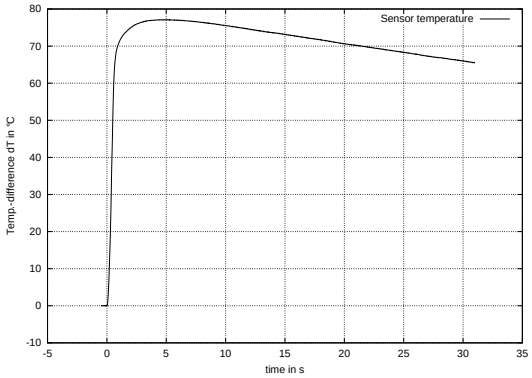


Figure 3: Calibration measurement of calorimeter temperature.

### 4.1 GAS TEMPERATURE DETERMINATION WITHOUT REGULARIZATION

For studying the expected effect of ill-posedness occurring with equation (13) we first test a discretized version of the least-squares fitting

$$\|F(G) - y^*\|^2_{L^2(0,t_{\text{end}})} \longrightarrow \min, \quad \text{subject to} \quad G \in D_{\text{box}} \tag{14}$$

with a box-constraints domain $D_{\text{box}}$ defined by inequalities of the form $0 \le G(t) \le G_{\max}$ for all times $t$ under consideration and a maximal temperature $G_{\max} = 8000K$. A solution $G_{ls}$ of the extremal problem (14) for our data $y^*$ is shown in Figure 4.

The peak of $G_{ls}(t)$ in a neighborhood of $t \approx t_p = 0.5s$ caused by the extreme energy of the electric arc seems to be approximated quite well. For times $t$ after this peak a temperature decay (first with a high and at the end with a low rate) occurs, but there we find strong oscillations of $G_{ls}$ in the cooling phase,

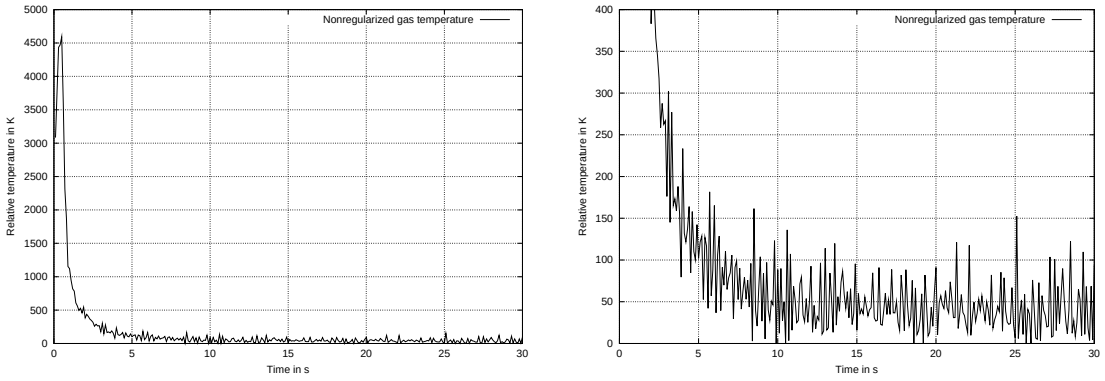


Figure 4: Gas temperature without regularization with zoom in the lower temperature interval.

which are not physically interpretable and obviously express ill-posedness phenomena. Such oscillations cannot be accepted in the approximate solution of $G$ for practical use, since forward computations of the arc test with real textile material seem to be more sensitive to gas temperature changes in the final phase of cooling. This is due to the fact that the thermal conductivity of the isolation material is much lower than in the simplified test situation used for solving the inverse problem.

### 4.2. A STANDARD TIKHONOV REGULARIZATION APPROACH

In order to overcome the drawback of ill-posedness, we should follow a regularization approach (cf., e.g., [1], [4]) for solving the operator equation (13) by a numerical procedure (see also [10]). Next instead of (14) we use a discretized version of the second order standard Tikhonov method solving the extremal problem

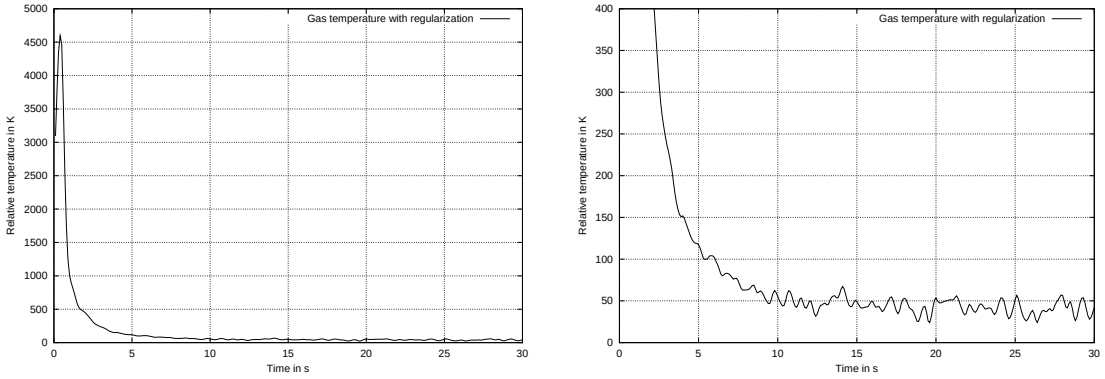


Figure 5: Gas temperature with second order Tikhonov regularization and zoom.

$$\|F(G) - y^*\|^2_{L^2(0,t_{\text{end}})} + \alpha \, \|G''\|^2_{L^2(0,t_{\text{end}})} \longrightarrow \min, \quad \text{subject to} \quad G \in D_{\text{box}} \tag{15}$$

with minimizer $G_\alpha$. For the selection of the regularization parameter $\alpha > 0$ we use the quasi-optimality criterion (see, e.g., [3, p.182]). In a sequence of parameters $\alpha_i = 2^{-i}\,\alpha_0$ with $\alpha_0 = 10^{-3}$ we have choosen $\alpha = \alpha_i$ such that $\|G_{\alpha_{i+1}} - G_{\alpha_i}\|_{L^2(0,t_{\text{end}})}$ is minimal, which is nearly the same as minimizing the norm of $\alpha \frac{dG_\alpha}{d\alpha}$. The resulting quasi-optimal $G_\alpha$ is shown in Figure 5. Oscillations also occur in the cooling phase, but they are less and smaller compared to the least-squares fitting. Note that the image function $F(G_\alpha)$ for that regularized solution is still a good approximation of the data function $y^*$.

We know the basic theoretical drawback (see, e.g., [1, Theorem 3.3]) of criteria for choosing the regularization parameter $\alpha$ that do not exploit the noise level $\delta$ satisfying $\|y - y^*\|_{L^2(0,t_{\text{end}})} \leq \delta$, but unfortunately the rapidly increasing temperature of the calorimeter (see Figure 3) in connection with temperatures up to 5000K near the arc and unknown inertia of the measurement system makes the prescription of a realistic $\delta$ required for the use of a discrepancy principle very problematic. On the other hand, the authors have good experience concerning the use of the quasi-optimality principle in very different practical applications.

### 4.3. A DESCRIPTIVE REGULARIZATION APPROACH

As third approach we use an ansatz of descriptive regularization. In detail, we add more a priori information about the qualitative behavior of the gas temperature function, in particular the knowledge of monotonicity expressed by a more restricted domain $D_{\mathrm{descr}} \subset D_{\mathrm{box}}$. During the burning time of the electric arc $t \in [0, t_p]$ we can assume a strictly growing function $G(t)$. On the other hand, for sufficiently large $t$, here $t \geq 2t_p$, we have a monotone decay of the gas temperature. For the gap interval $t \in (t_p, 2t_p)$ we do not impose additional requirements, but even for regularized solutions without monotonicity we have no oscillations in this time interval. The regularized solution $G_\alpha^{\mathrm{descr}}$ presented in Figure 6 is obtained by solving a discretized version of

$$\|F(G) - y^*\|^2_{L^2(0,t_{\mathrm{end}})} + \alpha \|G''\|^2_{L^2(0,t_{\mathrm{end}})} \longrightarrow \min, \quad \text{subject to} \quad G \in D_{\mathrm{descr}} \tag{16}$$

again based on a quasi-optimal choice of the regularization parameter $\alpha$. The values $G_\alpha^{\mathrm{descr}}(t)$ of this approximate solution are not very different from the values $G_\alpha(t)$ for small $t$, but by construction the function $G_\alpha^{\mathrm{descr}}$ suppresses oscillations nearly complete.

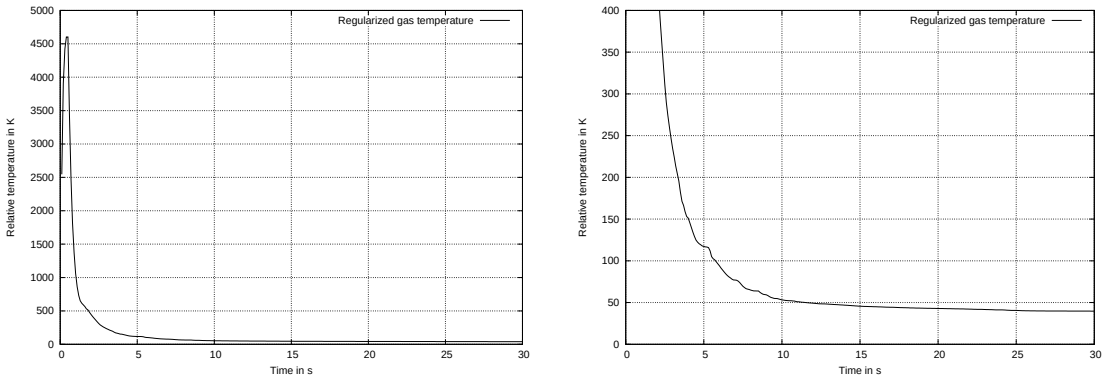


Figure 6: Gas temperature with descriptive regularization and zoom.

### 4.4. A SENSITIVITY STUDY

Finally we present a case study the purpose of which is to evaluate the system condition, i.e., the sensitivity of unregularized least-squares solutions with respect to data perturbations. Moreover, the influence of monotonicity requirements for that condition is investigated. In detail, we discretize our data function $y^*$ and perturb the obtained data vector $\underline{y}^*$ by a Gaussian pseudorandom vector $\underline{\varepsilon}$ such that normalized noise level $\frac{\|\underline{\varepsilon}\|}{\|\underline{y}^*\|}$ is $\delta > 0$. The vectors $\underline{G}^0_{ls}$ and $\underline{G}^\delta_{ls}$ are solutions for $\underline{y}^*$ and $\underline{y}^\delta = \underline{y}^* + \underline{\varepsilon}$, respectively, and $e^\delta_{ls} = \|\underline{G}^\delta_{ls} - \underline{G}^0_{ls}\|$ expresses the error caused by the data perturbation. Moreover, we repeat this procedure by considering monotonized solutions $\underline{G}^0_{\mathrm{mon}}$ and $\underline{G}^\delta_{\mathrm{mon}}$ with error $e^\delta_{\mathrm{mon}} = \|\underline{G}^\delta_{\mathrm{mon}} - \underline{G}^0_{\mathrm{mon}}\|$. The monotonized solutions are calculated from $\underline{y}^*$ and its perturbed counterpart by least-squares projections of data and approximate solutions onto the set of appropriate monotone functions, where monotonicity requirements are imposed similar to the situation described in Section 4.3. Figure 7 shows the monotonized solution $G^0_{\mathrm{mon}}$ which is rather similar to the regularized solution $G_\alpha^{\mathrm{descr}}$ of the last subsection, but the monotonized function is not so smooth as the descriptively regularized one.

Table 1 gives the ranges of relative errors over three realizations for solutions and their monotonized versions. The errors approximately behave proportional to $\sqrt{\delta}$, but the proportionality factor is essentially smaller for the monotonized version.

| $\delta$ | $\frac{e^\delta_{ls}}{\|\underline{G}^0_{ls}\|}$ | $\frac{e^\delta_{\mathrm{mon}}}{\|\underline{G}^0_{\mathrm{mon}}\|}$ |
|---|---|---|
| 0.05 | 0.6 ... 0.7 | 0.15 ... 0.21 |
| 0.01 | 0.32 ... 0.36 | 0.06 ... 0.11 |
| 0.005 | 0.2 ... 0.3 | 0.05 ... 0.08 |
| 0.001 | 0.11 ... 0.13 | 0.02 ... 0.03 |

Table 1: Sensitivity to data noise.

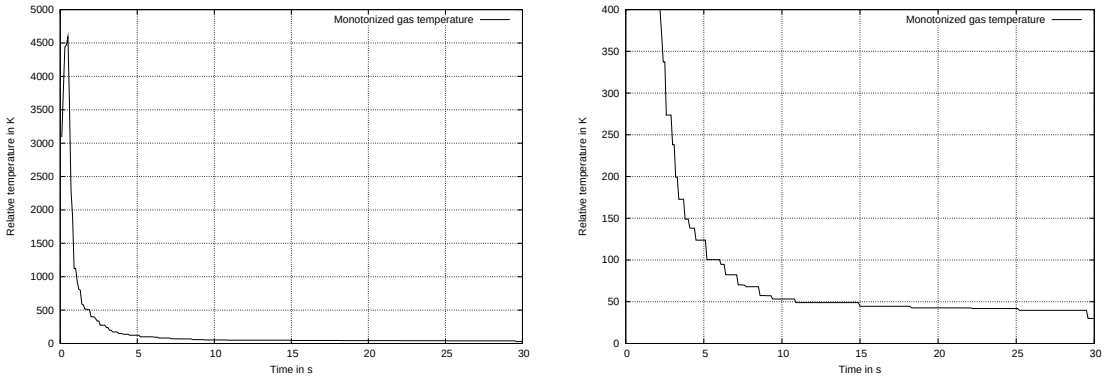


Figure 7: Monotonized gas temperature without regularization and zoom.

## 5. CONCLUSIONS

The presented mathematical model and numerical approach allow to simulate fault arc tests occurring in textile research concerning protective clothes. This computer simulation is very cheap in comparison with the traditional expensive laboratory experiments. The inverse problem of determining the time-dependent function of hot gas near the electric arc seems to play an important role for the success of the simulation. We have presented some case studies for the stable approximate solution of this inverse problem using various regularization techniques. Smoothness and monotonicity assumptions allow to suppress oscillations of recovered gas functions in the cooling phase.

## REFERENCES

1. H.W. Engl, M. Hanke and A. Neubauer, *Regularization of Inverse Problems,* Kluwer, Dordrecht, 1996.

2. A. Friedman, *Partial Differential Equations of Parabolic Type,* Prentice Hall, Englewood Cliffs, 1964.

3. P.C. Hansen, *Rank-Deficient and Discrete Ill-Posed Problems,* SIAM, Philadelphia, 1998.

4. B. Hofmann, *Regularization for Applied Inverse and Ill-Posed Problems,* Teubner, Leipzig, 1986.

5. M. Jakob, *Heat Transfer,* Volume I, John Wiley & Sons, New York, 1949.

6. International Social Security Association (ISSA), Section Electricity–Gas–Long-Distance Heating–Water, *Guideline for the selection of personal protective clothing when exposed to the thermal effects of an electric arc,* c/o Berufsgenossenschaft der Feinmechanik und Elektrotechnik, Köln, 2002.

7. O.A. Ladyženskaja, V.A. Solonnikov and N.N. Ural'ceva, *Linear and Quasilinear Equations of Parabolic Type,* American Mathematical Society, Providence, Rhode Island, 1968.

8. H. Schau and J. Haase, Electric Fault Arc Calorimetric Analysis based on ENV 50354:2000. *Proceedings of the 6th International Conference on Live Maintentance (ICOLIM 2002)* , VDE-Verlag, Berlin, 2002, pp.333-339.

9. P. Steinhorst, *Simulation of the Nonstationary Heat Transfer Through Heat Protecting Textiles* (in German). Diploma Thesis, University of Technology, Chemnitz, 2003.

10. C.R. Vogel, *Computational Methods for Inverse Problems,* SIAM, Philadelphia, 2002.